COULOMB-NUCLEAR INTERFERENCE POLARIMETER

Alain de Lesquen
Departement de Physique des Particules Elementaire
CEN-Saclay Gif-sur-Yvette (France)

(for the E581/704 collaboration*)

SUMMARY

At the end of the 87-88 fixed target period, some time was devoted to the absolute measurement of the polarization of the new high energy polarized proton beam which is to be used for the E704 experiment. Here we report on the test of a polarimeter based on the Coulomb Nuclear Interference (CNI) . Feasiblility of the method was established and, in the course of this test, improvements needed to increase efficiency and the precision became evident. Beam time was too limited to allow accurate verification of the beam polarization, but some corroboration of the tagging method was obtained for both protons and antiprotons.

UNDERLYING PRINCIPLE

Starting from an old idea of Schwinger[1], it was pointed out by Kopeliovich and Lapidus[2] and Buttimore et al.[3], that in pp elastic scattering at very small $|t|$ (between 0.001 and 0.020 $(GeV/c)^2$) there should be a small but significant analyzing power arising from the interference between the hadronic non-flip amplitude and the electromagnetic spin-flip amplitude.

In terms of helicity amplitudes we know that analyzing power can be expressed as follows;

$$A\frac{d\sigma}{dt} = -\mathrm{Im}\{(\Phi_1 + \Phi_2 + \Phi_3 - \Phi_4)\cdot\Phi_5\}$$

where each amplitude Φ_i is the sum of two components; the electro-magnetic part and the hadronic one, i.e.;

$$\Phi_i = \Phi_i^N + \Phi_i^{em}$$

At very small t-values three of the five hadronic amplitudes vanish and the optical theorem allows the sum of the imaginary part of the two remaining components to be computed from the known total cross section, i.e.;

$$\Phi_2^N = \Phi_4^N = \Phi_5^N = 0.$$

$$\mathrm{Im}(\Phi_2^N + \Phi_3^N) = \frac{[s(s-4m^2)]}{4\pi}\sigma_{tot}$$

The analyzing power arises mainly from the interference between electromagnetic and hadronic amplitudes, i.e.;

$$A\frac{d\sigma}{dt} = -\mathrm{Im}\{(\phi_1^N + \phi_3^N)\phi_5^{em*}\}$$

Since the electromagnetic amplitude can be calculated, e.g. using the one- photon exchange approximation;

$$\Phi_5^{em} = \frac{\alpha\sqrt{s}}{\sqrt{|t|}}\cdot\{\frac{\upsilon-1}{2m} + O(t)\}$$

The analyzing power is therefore a known function of total cross section and momentum transfer, with a maximum of A_m at $t = t_m$, and a shape (see fig. 1) given by;

$$A = A_m\cdot\frac{4z^{3/2}}{3z^2 + 1}$$

with

$$z = \frac{t}{t_m}$$

$$t_m = \sqrt{3}.(8\pi\alpha/\sigma_{tot})$$

$= .0032\ (\mathrm{GeV/c})^2$ (for $\sigma_{tot} = 39$ mb)

$A = \sqrt{3/4}(\upsilon - 1)(\sqrt{t_m}/m) = 4.6\ \%$

APPARATUS

(a) Beam

The E704 beam is described in more detail elsewhere [4]. This beam is a secondary beam with a central momentum of 185 GeV/c and a momentum spread of ± 9%. A spectrometer in the beam measured the momentum of each particle to ± 1.5%. The beam consists of protons ($\bar{p}$'s) produced from decay of Λ's ($\bar{\Lambda}$'s) generated by the incidence of the 1 TeV primary beam on a production target. It is well known that such protons are longitudinally polarized (at 64%) when seen in the centre of mass of the

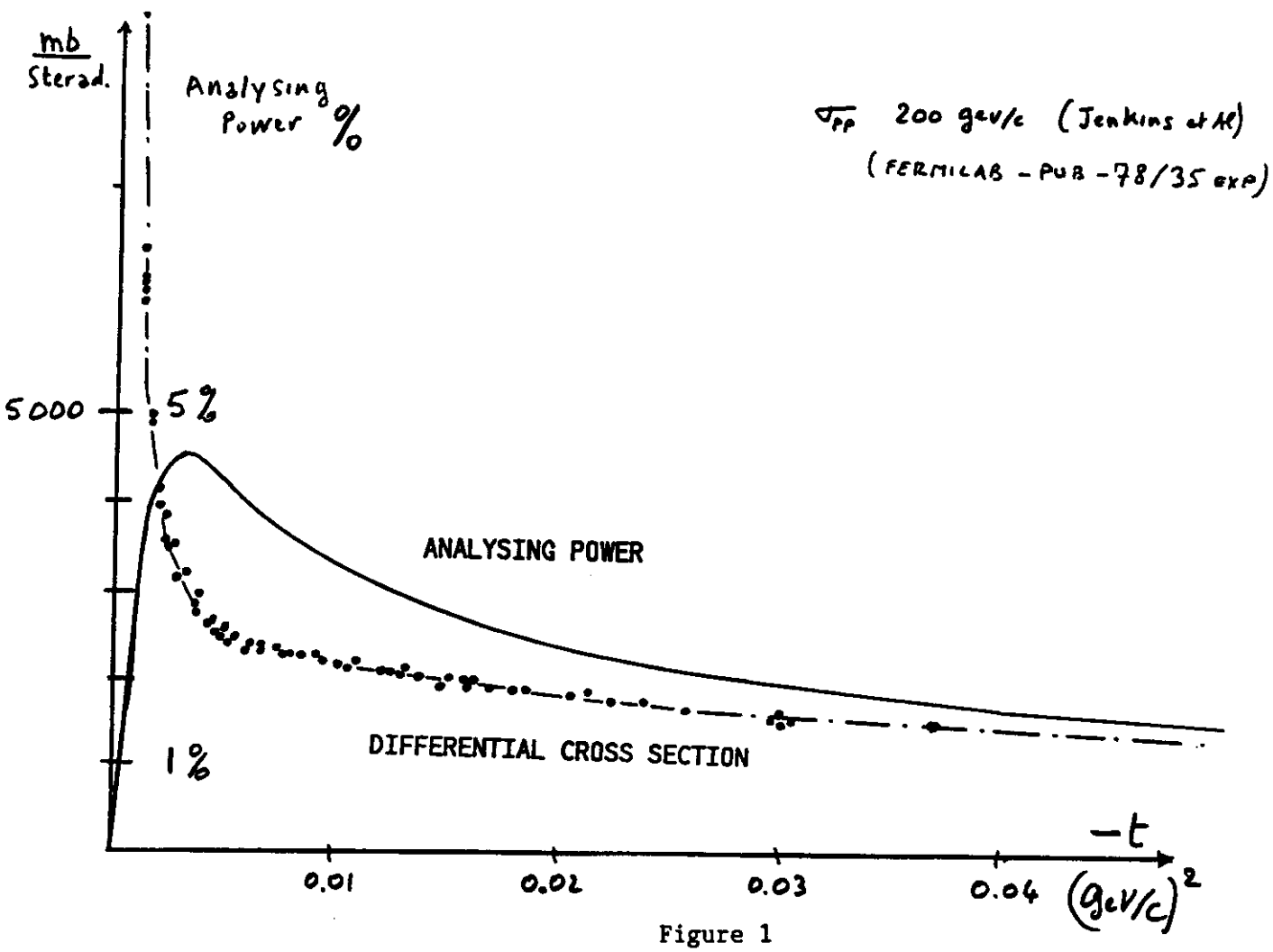

Figure 1

Λ. If we select events which decay at 90° relative to the line of flight of the lambda , taking account of the Lorenz boost introduced by the momentum of the Λ, we obtain a transversely polarized proton beam. In our case Λ-decays with the proton in the horizontal plane are used, so that the resulting polarization also lies in the horizontal plane and has a rather flat polarization distribution ranging from -64% to 64%. As different polarization values have different phase space, the horizontal position of the protons at the intermediate focus of the beam is directly related to the polarization of each particle. This relation (position vs. polarization) has been determined by Monte-Carlo generation, and allows us to assign a "polarization value" (within ± 5%) for each proton.

An absolute calibration of the polarization is needed in order to check this calculation. Deviations could originate from contamination by unpolarized (or differently polarized) protons, or depolarization along the beam line. This depolarization is expected to be small because the magnetic dipoles and quadrupoles are arranged in pairs, symmetrically on each side of the intermediate focus, so that the precessions of spins in the magnets of the first half of the beam are cancelled out in the magnets of the second half.

A spin rotator (also referred to as a Siberian Snake), situated towards the end of the beam-line and is used to change the spin direction. It consists of 12 dipole magnets which allow one to rotate the polarization from the horizontal to the vertical or longitudinal direction, and to flip the orientation along these two directions while leaving the phase space unchanged. The orientation is usually flipped every ten beam spills. Pion contamination (due mainly to K decays) is eliminated by two Cerenkov counters in the beam. This contamination is 15% (85%) of the beam for protons (antiprotons).

(b) Targets

The polarimeter target was a set of 7 scintillation counters centered on the beam and separated by 20 cm (see fig.2). Thicknesses range between 0.5 and 5 mm. They are made of Pilot B except for the thickest one, which was a 5mm-thick Stilbene crystal ($C_{14}H_{12}$). The charge integral from each of their signals is recorded by ADC's in order to discriminate between passing particles, and particles which scattered at very low momentum from

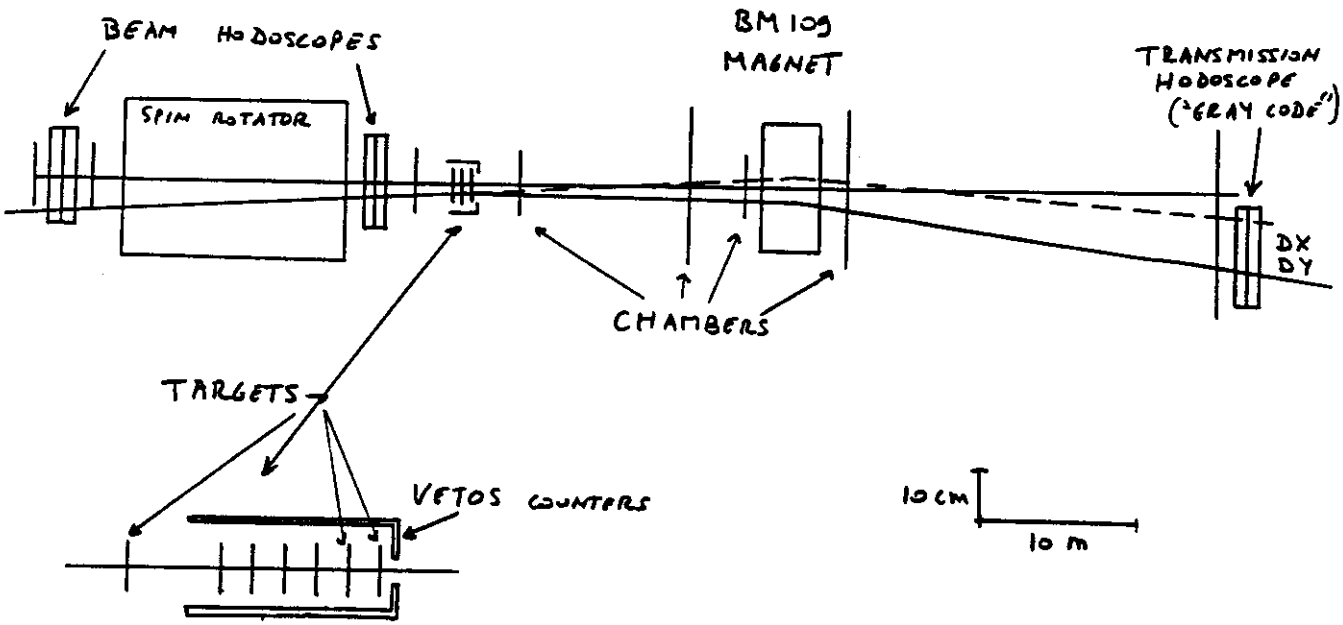

Figure 2

the free protons of the scintillator material. In this case the recoil proton has a small energy (a few MeV) and moves very nearly perpendicularly to the incident trajectory so that it stops within a very short range (~1 mm) in the scintillator itself. The energy deposited by the recoil proton adds to the energy deposited by the fast particle and there is therefore approximately a linear correlation between the ADC's recorded value and the momentum transfer squared $|t|$ of the scattered particle. This correlation is used to select elastic events. Unfortunately there is an appreciable probability of having a large pulse height without any scattering due to the weighting of the Landau distribution towards higher pulses heights [5].

Veto counters, (scintillator/lead sandwiches) are arranged around the targets to eliminate inelastic events generating charged particles, pi zeros and/or Gammas. They cover a solid angle of almost 4π steradian.

(c) Detectors

At the intermediate focus ("tagging station") a set of five hodoscopes are used to measure the momentum (3 horizontal hodoscopes) and the "polarization" (2 vertical hodoscopes) of each beam particle. Two more double hodoscopes (X and Y), situated at either end of the spin rotator, (see fig. 2) were used to determine the direction of incident particle. They consist of 14 (16) 3 mm thick, 1/3 overlapping scintillators of 10 (6) mm wide strips, resulting in a resolution of 3.3 (2) mm. A transmission hodoscope (also X and Y) is situated 48 m downstream of the targets to detect the scattered particle. It consists of five scintillators arranged in a pattern such that the outputs give directly the encoded position of the passing particle. Another set of five scintillators, in complementary positions, should give the complementary (i.e. exchanging 0 and 1) encoded position if only one particle is present. This characteristic is used to reject multiple tracks. Also, because the encoded position is in Gray code instead of normal binary code, an error in one of the five pairs can lead to an error of only one bin position[6]. This hodoscope covers 16 cm in 32 bins of 0.5 cm. A set of multiwire proportional chambers (MWPC's) are situated before and after the targets to measure the scattering angle. Together with a dipole magnet (2.66 tesla.m) situated 20 meters downsteam the targets, they allow a measurement of the scattered particle momentum to better than 1 %.

With this apparatus the total acceptance for the scattering angle is 1.7 milliradian. It corresponds to $|t| = 0.1$ $(GeV/c)^2$ for a beam momentum of 185 GeV/c. The angular resolution is of the order of 0.04 milliradian. The following table gives the experimental resolution for various value of the momentum transfer:

|t| + resol. (GeV/c)**2	Theta milliradian	Recoil energy MeV	Recoil Range mm (d = 1 g/cm3)
0.0010 + 0.0005	0.17 + 0.04	0.5	0.02
0.0030 + 0.0009	0.30	1.6	0.10
0.0100 + 0.0015	0.54	5.3	1.0
0.0300 + 0.0027	0.94	16.0	5.0
0.1000 + 0.0049	1.71	53.0	30.0

DATA TAKING : TRIGGER

The event selection at the fast trigger level, is done using only scintillators and hodoscopes along the trajectories.

The fast trigger requires:

=> One and only one incident particle seen by all the hodoscopes and no signal in the two beam Cerenkov.

=> At least one of the scintillating targets with a signal greater than the discrimination threshold. This threshold is set for each target so as to accept 5 % of the Landau distribution.

=> No hits in vetoes surrounding targets.

=> A kick in the transmission hodoscope ("Gray-Code") corresponding approximately to -t > 0.001 (GeV/c)**2

The signals corresponding to all these conditions were not fast enough to be used in the signal which initiated encoding of the ADC's and MWPC's so that we had to have a two step trigger logic ie.;

$$\text{PRETRIGGER} = GH*GB*TB*(\text{Target.OR})*\overline{\overline{\text{VETO}}*\overline{C}}$$

where;

GH = Good Hit = One and only one hit in the Tagging Hodoscopes

GB = Good Beam = One or more hits in the beam hodoscopes

TB = Transmitted beam = One or more hits in the transmission hodos

C = Cerenkov = not pions

This PRETRIGGER started the encoding cycle for the MWPC's and the ADC's. The Master trigger was then formed by incorporating a threshold condition

on scattering angle as calculated by MLU's as well as the information from the tagging station (which also arrived too late to be incorporated in the pretrigger), i.e.;

MASTER TRIGGER = PRETRIGGER*GT*[MLU logic]

where;

GT=Good Tagging = Only one hit in the Tagging Hodoscopes
[MLU logic] = Hardware calculation of scattering angles

The [MLU logic] computes the projection of the incident track, defined by beam hodoscopes, on the transmission hodoscope. The result is compared with the value measured by this last hodoscope. If the difference between these two values is sufficiently small (see below) the particle is considered undeviated and the event is rejected. The conditions governing this decision differed for the two data-taking perioids (Dec. 87 and Jan 88). If DX and DY are the horizontal and vertical projections of this difference, then;

for Dec. 87;		DX > 1.56 cm.	.OR.	DY > 1.28 cm.
for Jan. 88;	4 cm.	DX > 1.40 cm.	.AND.	DY < 0.83 cm.

i.e.,in the Jan. run, only events which scattered close to the horizontal plane, where the asymmetry is maximal for a vertically polarized beam, were accepted because of limitations in the data-acquisition rate. Notice that a scattering of $-t=0.001$ $(GeV/c)^2$ corresponds to D = 0.81 cm at an incident momentum of 185 GeV/c .

The data are read through CAMAC by a PDP11, and written on tape. A VAX can sample some of these events on-line and perform a partial or complete analysis. The on-line analysis is useful for monitoring the performance of both beam and the apparatus.

DATA ANALYSIS

All the events recorded on tape were analysed off-line on a VAX 780. Events for which the information from the "tagging Station" and hodoscopes were inconsistent and events for which the spin rotator was in an

indefinite status (2 spills out of 12) were rejected. So were events with a bad chambers efficiency, or high multiplicity.

(a) Tracking and vertex reconstruction

For the remaining events the charged particle track is reconstructed using the hodoscopes and the chambers. Multi-track events are rejected. The measured momentum in the forward spectrometer is expected to match the momentum given by the Tagging hodoscopes within 8 GeV/c (4.3 %) to ensure that it is compatible with an elastic scattering.

Track reconstruction is relatively easy as only one track is expected so that a sophisticated pattern recognition program is not needed. The rough tracks defined by the hodoscopes are used to define "useful" parts of each chamber in order to save computer time by reducing the number of candidate hits reconstruction of the scattered proton trajectory. Space along the beam axis is divided into three intervals where straight tracks are reconstructed independently; upstream of the target (beam), between the target and the BM109 magnet (scattered) and downstream the magnet (analyzed). An overall fit is then used to readjust the parameters assuming that these elementary straight tracks represent the trajectory of a real particle and must therefore intersect. The vertex is the reconstructed intersection point between the beam track and the scattered one. The four-momentum is computed from the deviation between the scattered and analyzed tracks and its value is correlated with the target ADC's.

(b) Targets signals

Two types of targets are used in the experiment: Six standard plastic scintillators with thicknesses 0.5-, 1.0-, 2.0- mm , and a 5.0- mm thick stilbene crystal. Signal-processing and analysis differs with the scintillator type.

(i) Plastic scintillators targets

For each event, the signal from each target is integrated and digitized by an ADC. Ideally, only one of these signals (the one corresponding to an elastic scattering) exceeds the discriminator

threshold. However due to the weighting of the Landau distribution towards the higher amplitudes, there is a significant probability that more than one threshold will be exceeded. It is assumed that the scattering took place in the scintillator corresponding to the largest signal.

Vertex definition is poor (+/- 50 cm half width) because of the very small scattering angles involved. A target spacing of 20 cm and the proximity of a hodoscope and definition counters used for beam tuning (total mean thickness 15 mm) makes it difficult to identify individual targets in the Z-vertex distribution. These centroids are identified by using kinematic cuts, after which a +/- 100cm cut around these centroids is used to reject background.

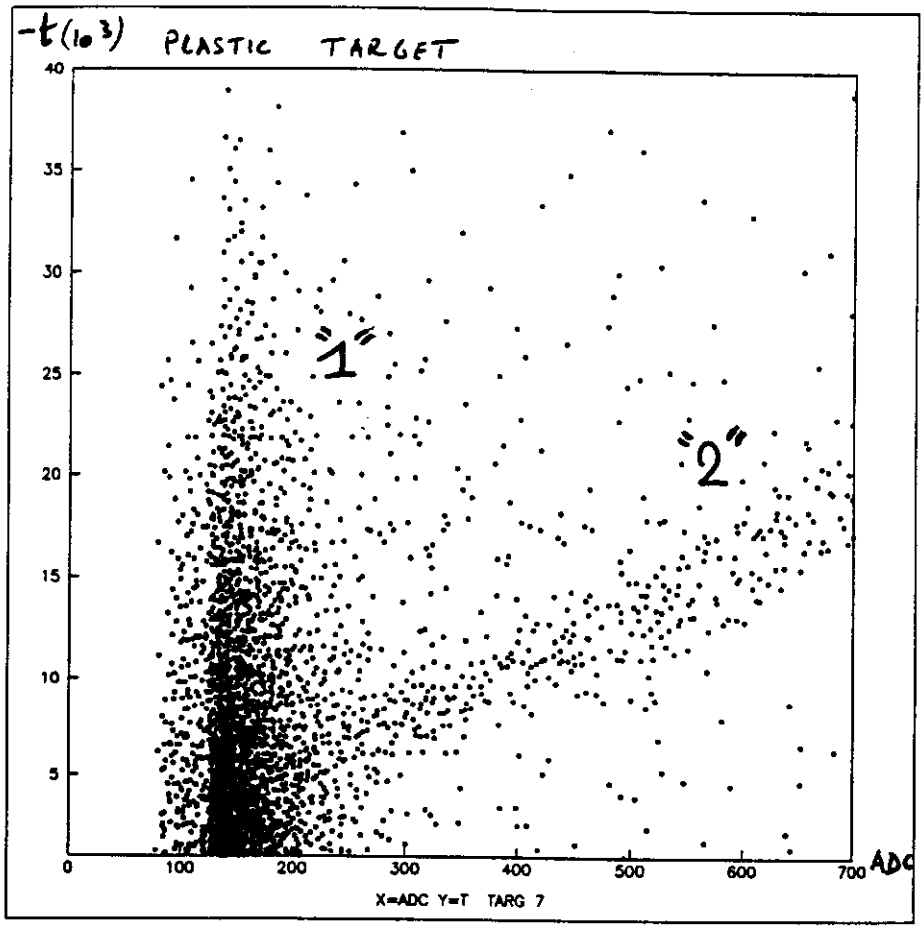

Figure 3

The two-dimensional plots $|t|$ versus pulse amplified (ADC) for each target have two distinguishing features (fig.3).

"1" An accumulation of low-amplitude events having no correlation with t. These correspond mainly to cases where the signal from a non-interacting particle exceeds threshold because of the Landau tail.

"2" Events which exhibit a clear, approximately linear correlation. These events correspond to elastic scattering from free protons in this target. The ADC's record the energy deposited by the recoil proton plus the energy deposited by the minimally-ionizing fast particle. These events are well separated from the uncorrelated background above some threshold. This theshold corresponds to a value of $|t|$ which increases with the thickness of the target, i.e.=0.003, 0.004 and 0.006 $(GeV/c)^2$ for 0.5, 1.0 and 2.0 mm.-thickness, respectively. These values are close to the expected ones [7].

(ii)Stilbene

Stilbene is an organic crystal scintillator for which the shape (decay time) of the signal depends of the ionisation density [8]. This particularity is used to discriminate between the minimally-ionising non-interacting protons and low-energy recoil protons, for which the signal has a relatively large slow component.

Two ADC's look at the signal: the first one ("total") integrates the full signal, and the second one ("slow") is gated so as to start integration 30 ns after the leading edge so that it integrates only the slow component. By comparison to the other targets, therefore the additional information allows better selection of elastic event at very low $|t|$. This is evident from the two dimensional plots "slow" versus "total" in which one distinguishes three regions (fig.4);

from bottom to top, one can see;

"1" a cloud of points for large "slow" values. These are either due to pile-up when a second particle arrives several tens of nanoseconds after the normal one, or to some nuclear effect which induces a delayed signal.

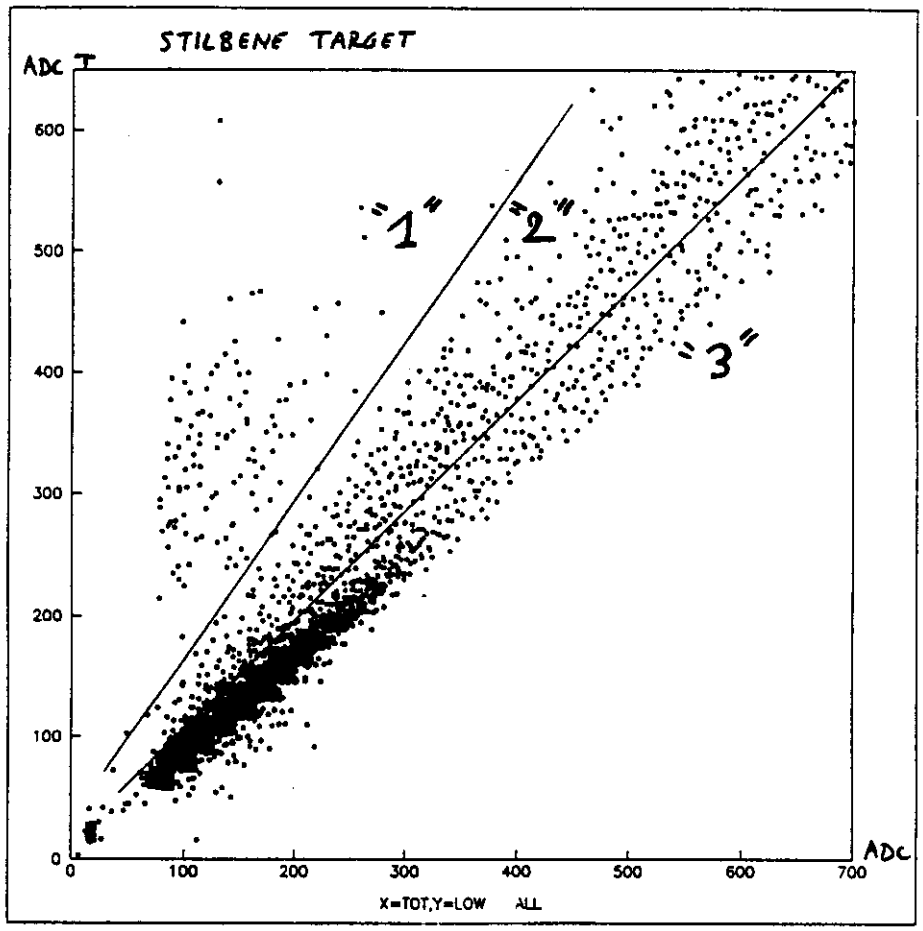

Figure 4

"2" a locus which corresponds to elastic scatterings, for which the slow integral (vertical axis) is relatively large.

"3" a second locus,clearly separated from the first, which corresponds to the Landau tail from non-interacting particles.

The Z-vertex distribution (fig. 5) shows a very strong correlation with the Stilbene position when only events of type "2" are selected. These elastic events are very well separated from type "1" events down to -t=0.002 (GeV/c)**2. The stilbene scintillator shows, at very low t, better separation than a 0.5 mm standard scintillator and gives a counting rate ten time greater.

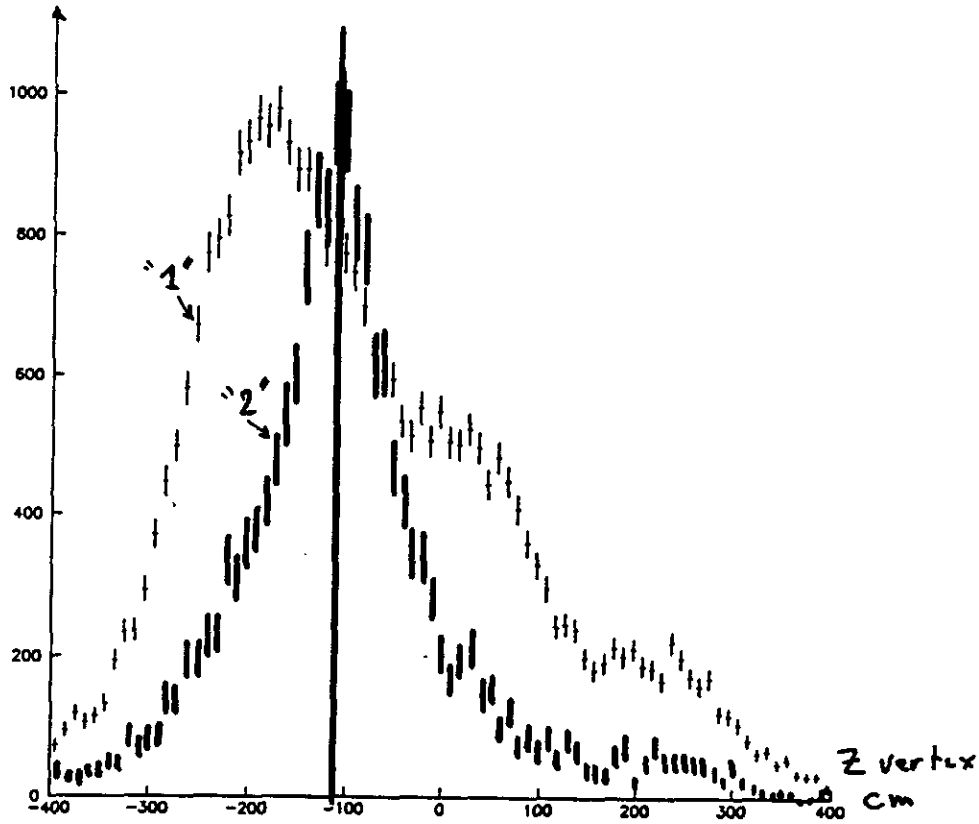

Figure 5

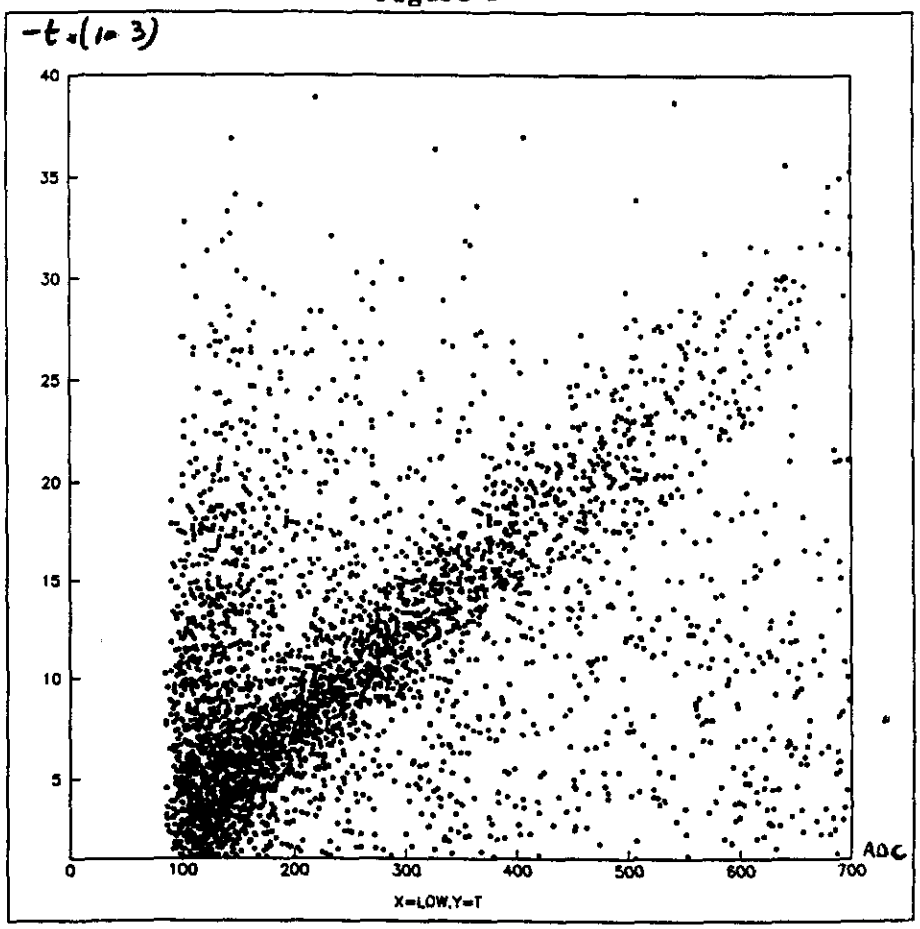

Figure 6

RESULTS

We ran for 6 days in three 48-hour periods in December 87 and January 88. The main part of the time was devoted to debugging and set-up. The total number of events recorded was 1,770,000 in 12 hours of data-taking in Dec. 87, with the first type of trigger, and 1,200,000 in 17 hours with the second type in Jan. 88. Of these these $3.0*10^6$ events, $0.6*10^6$ (20%) were identified as elastic scattering with a $|t| > 0.001$ $(GeV/c)^2$. The constraint corresponding to this $|t|$- threshold gave the main rejection factor (55% of events being due to non-interacting protons, very small-angle scattering or elastic scattering from carbon). The principal reason for such a large number of such events being passed by the trigger was the smearing in the dispersion introduced by BM109 due to the momentum spread of the beam. This introduced a corresponding smearing in the horizontal position on the "Gray-Code" hodoscope which was situated downstream the analyzing magnet. The second most important cause of rejection was the inconsistencies in the "tagging" information, beam hodoscopes and the "gray-Code" hodoscopes (multiplicity, "impossible track", momentum out of range, etc).

The beam polarization distribution is expected to be flat between -64% and 64%. Neglecting those events with a $|t| > 0.03$ $(GeV/c)^2$ (small analyzing power -- see fig.1) We distinguished between three different categories depending of the beam polarization P_b measured by the tagging system, i.e. $|P_b| > 30\%$, $10 < |P_b| < 30$ % and $|P_b| < 10\%$. The asymmetries are calculated for these three different categories , and taking account of the average of the analyzing power in the interference region (3.7% -- see fig. 1), the beam polarization was deduced in each case. Unfortunately , though it was easy to extract a pure elastic scattering events from the correlation between $|t|$ and the ADC reading, the number of such events (18000 to 20000) is too small to allow a statistically significant numerical result. Only the sign of the beam polarization could be verified, i.e.;

$$P_b = \mathbf{41.} \pm \mathbf{25.} \quad \text{(expected 42.0\%)}$$

The events which did not satisfy the correlation between amplitude and t are either events which scattered from free proton of other scintillators, or events which scattered elastically on carbon nuclei (with comparable analyzing power). Including these events in the calculation of the asymmetry and assuming the same analyzing power, we obtain results which are compatible with the hypothesis of a slightly diluted analysing power, i.e.: as calculated by Buttimore in reference 9:

category	measured $\langle P_b \rangle$	
$30 < \lvert P_b \rvert$	22.3 ± 7.7	(expected 41.5) %
$10 < \lvert P_b \rvert < 30$	20.5 ± 9.2	(18.1) %
$\lvert P_b \rvert < 10$	2.0 ± 12.3	(0.0) %

For down/up asymmetries we obtain;

category	measured $\langle P_b \rangle$
$30 < \lvert P_b \rvert$	-5.9 ± 10.5 %
$10 < \lvert P_b \rvert < 30$	6.1 ± 12.7 %
$\lvert P_b \rvert < 10$	14.8 ± 17.1 %

This is consistent with an expected down/up asymmetry of zero for a vertical orientation of the beam polarization.

ANTIPROTONS

At the end of the fix-target run two hours of data with the polarized anti-proton beam were taken. Very few events which scattered from the CNI targets were recorded, but a 15 cm-long CH_2 target was set up downstream of the scintillation targets from which a significant number of small-angle scatterings were rercorded. Ignoring the information from the target ADC's, 60000 small-angle scattering events were extracted from 127000 triggers. The beam polarization calculated from these events, assuming exactly the same analyzing power for inclusive small-angle scattering of antiprotons as we did for inclusive small-angle proton scattering, was consistent with the expected value of beam polarization;

category	measured $\langle P_b \rangle$	
$30 < \lvert P_b \rvert$	41.9 ± 16.8	(expected 41.7) %
$10 < \lvert P_b \rvert < 30$	30.6 ± 18.9	(18.6) %

CONCLUSION

The results, although of limited significance due to the low statistics, are consistent with expected beam polarisation. Of more significance, is that we have demonstrated that the method can be used successfully to measure the polarization of high energy polarized beam. This test has suggested several improvements in the apparatus and in the trigger logic. The main improvement will be the use of 3 or 5 mm thick Stilbene targets instead of the very thin plastic scintillation targets. This will increase the rate of acquisition of elastic scatering events, especially at low $|t|$, and simplify analysis as the ratio signal over background is better. Application of the polarimeter to the measurement of the E704 beam polarization is expected during the next fixed target period.

* The E-581/704 Collaboration: N. Aktchurin[1], D. Carey[2], R. Coleman[2], M. Corcoran[11], D. Cossairt[2], A. Derevschikov[3], D. P. Grosnick[4], M. M. Gazzaly[5], D. Hill[4], K. Imai[6], M. Laghai[4], F. Lehar[7], A. deLesquen[7], D. Lopiano[4], F. C. Luehring[8], K. Kuroda[9], A. Maki[10], A. Masaike[6], Yu. A. Matulenko[3], A. P. Meschanin[3], A. Michalowicz[9], D. H. Miller[8], K. Miyake[6], T. Nagamine[6], F. Nessi-Tedaldi[11], M. Nessi[11], C. Ngugen[11], S. B. Nurushev[3], Y. Ohashi[4], Y. Onel[1], G. Pauletta[12,13], A. Penzo[14], G. C. Phillips[11], A. L. Read[2], J. B. Roberts[11], L. vanRossum[7], G. Salvato[15], P. Schiavon[14], T. Shima[4], V. L. Solovyanov[3], H. Spinka[4], R. W. Stanek[4], R. Takashima[6], F. Takeuchi[6], N. Tanaka[16] D. G. Underwood[4], A. N. Vasiliev[3], A. Villari[15], J. White[11], A. Yokosawa[4], T. Yoshida[6], A. Zanetti[14]

1 Department of Physics, University of Iowa, Iowa City, IA 52242, USA.
2 Fermi National Accelerator Laboratory, Batavia, IL 60510, USA.
3 Institute of High Energy Physics, Serpukhov, USSR.
4 Argonne National Laboratory, Argonne, IL 60439, USA.
5 Department of Physics, University of Minnesota, Minneapolis, MN 55455, USA.
6 Kyoto University, Kyoto 606, Japan.
7 SEPh-DPhPE, CEN-Saclay, F-91191 Gif Sur Yvette Cedex, France.
8 Physics Department, Northwestern University, Evanston, IL 60201, USA.
9 LAPP, BP 909, 74017 Annecy-le-Vieux, France.
10 University of Occupational and Environmental Health, Kita-Kyushu, Japan.
11 T. W. Bonner Nuclear Laboratory, Rice University, Houston, TX 77251 USA.
12 Physics Department, University of Texas, Austin, TX 78712, USA
13 Institute of Physics, University of Udine, 33100 Udine, UD, Italy.
14 INFN and University of Trieste, I-34100, Trieste, Italy.
15 University of Messina, Messina, Italy.
16 Los Alamos National Laboratory, Los Alamos, NM 87545, USA.

REFERENCES

1) J. Schwinger, Phys. Rev. 73, 407 (1948).

2) B. Z. Kopeliovich and L. I. Lapidus, Sov. J. Nucl. Phys. 19, 114 (1974).

3) N. H. Buttimore, E. Gotsman and E. Leader, Phys. Rev. D18, 694 (1978).

4) See the communications of D. Underwood and L. Coleman in this proceeding.

5) H. Azaiez et al., in "Miniaturization of High Energy Physics Detectors" edited by A. Stephani (Plenum Publishing Corporation 1983), and H. Azaiez et al., "Calibration and Monitoring of High Energy Polarized Beam... (unpublished).

6) M. Arignon et al., Nucl. Instrum. and Meth., A235, 523 (1985). Note that the Gray code counter described in this reference is circular whereas, two (x and y) linear ones were used in this experiment.

7) K. Kuroda , A. Penzo and V. Solovyanov, CERN-EP internal report 79-1 (unpublished)>

8) J. B. Birks in "The Theory and Practice of Scintillation Counting", London (1967).

9) N. H. Buttimore, Proceedigs of the High Energy Spin Physics Conference, Brookhaven 1982, edited by Gerry M. Bunce, New York, American Institute of Physics (1983).